J|A|C|S
ARTICLES

Published on Web 03/10/2009

cis-β-Bis(carbonyl) Ruthenium−Salen Complexes: X-ray Crystal Structures and Remarkable Catalytic Properties toward Asymmetric Intramolecular Alkene Cyclopropanation

Zhen-Jiang Xu,[†] Ran Fang,[‡] Cunyuan Zhao,[‡] Jie-Sheng Huang,[§] Gong-Yong Li,[†] Nianyong Zhu,[§] and Chi-Ming Che*[,†,§]

Shanghai−Hong Kong Joint Laboratory in Chemical Synthesis, Shanghai Institute of Organic Chemistry, The Chinese Academy of Sciences, 354 Feng Lin Road, Shanghai 200032, MOE Key Laboratory of Bioinorganic and Synthetic Chemistry, School of Chemistry and Chemical Engineering, Sun Yat-Sen University, Guangzhou 510275, and Department of Chemistry and Open Laboratory of Chemical Biology of the Institute of Molecular Technology for Drug Discovery and Synthesis, The University of Hong Kong, Pokfulam Road, Hong Kong, People's Republic of China

Received November 7, 2008; E-mail: cmche@hku.hk

Abstract: *cis*-β-[Ru^{II}(salen^{A})(CO)$_2$] (salen^{A} = *N*,*N*′-bis(3-R^1-5-R^2-salicylidene)-1,2-cyclohexenediamine dianion; $R^1 = R^2 = Bu^t$, **1a**; $R^1 = Pr^i$, R^2 = H, **1b**; $R^1 = Bu^t$, R^2 = H, **1c**) complexes were prepared by treating $Ru_3(CO)_{12}$ with the respective H_2salen^{A} in 1,2,4-trichlorobenzene and structurally characterized by X-ray crystallography. Complexes **1a**−**c** catalyze intramolecular cyclopropanation of *trans*-allylic diazoacetates $N_2CHCO_2CH_2CH{=}CHR$ (**3**, R = Ph, 4-ClC_6H_4, 4-BrC_6H_4, 4-MeC_6H_4, 4-$MeOC_6H_4$, 2-MeC_6H_4, 2-furanyl) under light irradiation to give cyclopropyl lactones **4** in up to 96% yield and up to 98% ee. DFT calculations on intramolecular cyclopropanation of **3a** (R = Ph) with model catalyst *cis*-β-[Ru^{II}(salen^{A0})(CO)$_2$] (salen^{A0} = *N*,*N*′-bis(salicylidene)-1,2-cyclohexenediamine dianion) reveal the intermediacy of both *cis*-β- and *trans*-[Ru(salen^{A0})($CHCO_2CH_2CH{=}CHPh$)(CO)] bearing salen^{A0} in a nonplanar and planar coordination mode, respectively, with the *cis*-β-carbene species being a major intermediate in the catalytic carbenoid transfer reaction. The intramolecular cyclopropanation from the *cis*-β-carbene species is the most favorable pathway and features an early transition state and an asynchronous concerted [2 + 1] addition mechanism. Enantioselectivities in the reactions involving [Ru(salen^{A0})($CHCO_2CH_2CH{=}CHPh$)(CO)] were predicted to be 77% ee for the *trans*-carbene species and 96% ee for the *cis*-β-carbene species; the former dramatically increases to 98% ee, whereas the latter slightly increases to 99% ee, upon replacing salen^{A0} with salen^{A1} ($R^1 = R^2 = B^t$). The observed variation in enantioselectivity (90−98% ee) for the conversion of **3a** to **4a** catalyzed by **1a**−**c** could result from an equilibrium between *cis*-β (major) and *trans* (minor) ruthenium−carbene intermediates.

Introduction

Tetradentate N_2O_2 salen ligands formed from salicylaldehydes and 1,2-diamines, herein denoted as salen^{A} (Figure 1), have been widely used in coordination chemistry and catalysis.[1] Numerous metal complexes of such salen ligands are known in the literature, either isolated in pure form or generated in situ. It is usually considered that these complexes contain planar salen^{A} ligands; that is, the salen^{A} N_2O_2 atoms coordinated to a metal ion are basically coplanar, as depicted in the *trans* configuration of an octahedral complex in Figure 1, regardless of whether the salen^{A} skeleton adopts a stepped or umbrella conformation.[1g−i,l] The planar salen^{A} coordination serves as a basis on which various reaction intermediates in related catalytic processes are proposed,[1a,c,g,j−m] including the chiral intermediates responsible for the enantioselectivity in asymmetric catalysis.[1a,c,g,l,m]

A nonplanar salen^{A}, herein defined as the coordinated salen^{A} ligand adopting a nonplanar N_2O_2 geometry, is not unprecedented but remains sparsely seen in the literature and has been confirmed, by X-ray crystal structure determination, only for the complexes containing either bidentate co-ligands or a few d^0 transition metal ions (such as Ti^{IV}, Zr^{IV}, Hf^{IV}, W^{VI}, and Mo^{VI}),[1] in which cases a *cis*-β configuration depicted in Figure

[†] Shanghai Institute of Organic Chemistry.
[‡] Sun Yat-Sen University. Correspondence on the DFT calculations described in this paper should be addressed to Cuanyuan Zhao.
[§] The University of Hong Kong.

(1) For recent reviews, see: (a) Katsuki, T. *Coord. Chem. Rev.* **1995**, *140*, 189. (b) Yamada, S. *Coord. Chem. Rev.* **1999**, *190*−*192*, 537. (c) Jacobsen, E. N. *Acc. Chem. Res.* **2000**, *33*, 421. (d) Atwood, D. A.; Harvey, M. J. *Chem. Rev.* **2001**, *101*, 37. (e) Kojima, M.; Taguchi, H.; Tsuchimoto, M.; Nakajima, K. *Coord. Chem. Rev.* **2003**, *237*, 183. (f) Tsuchida, E.; Oyaizu, K. *Coord. Chem. Rev.* **2003**, *237*, 213. (g) Katsuki, T. *Synlett* **2003**, 281. (h) Cozzi, P. G. *Chem. Soc. Rev.* **2004**, *33*, 410. (i) Katsuki, T. *Chem. Soc. Rev.* **2004**, *33*, 437. (j) Darensbourg, D. J.; Mackiewicz, R. M.; Phelps, A. L.; Billodeaux, D. R. *Acc. Chem. Res.* **2004**, *37*, 836. (k) Venkataramanan, N. S.; Kuppuraj, G.; Rajagopal, S. *Coord. Chem. Rev.* **2005**, *249*, 1249. (l) McGarrigle, E. M.; Gilheany, D. G. *Chem. Rev.* **2005**, *105*, 1563. (m) Baleizão, C.; Garcia, H. *Chem. Rev.* **2006**, *106*, 3987. (n) Matsumoto, K.; Saito, B.; Katsuki, T. *Chem. Commun.* **2007**, 3619.

(2) (a) Herrmann, W. A.; Rauch, M. U.; Artus, G. R. J. *Inorg. Chem.* **1996**, *35*, 1988. (b) Munslow, I. J.; Gillespie, K. M.; Deeth, R. J.; Scott, P. *Chem. Commun.* **2001**, 1638. (c) Knight, P. D.; Scott, P. *Coord. Chem. Rev.* **2003**, *242*, 125. (d) Che, C.-M.; Huang, J.-S. *Coord. Chem. Rev.* **2003**, *242*, 97.

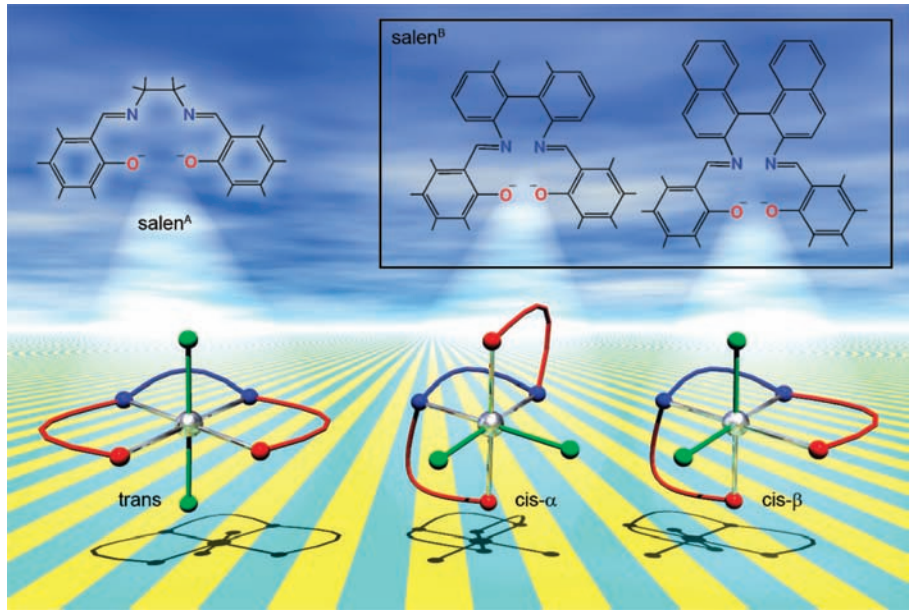

Figure 1. Schematic diagram showing the possible coordination modes of salens in their octahedral metal complexes.

1 is observed. Notably, replacement of the two-carbon bridge (between the salen N atoms) of salen^A by a longer carbon chain[2a] or a biaryl group[2b−d] changes the salen coordination from planar to nonplanar. The octahedral complexes of biphenyl or binaphthyl salens, herein denoted as salen^B (inset of Figure 1), are reported to prefer *cis*-α and *cis*-*β* configurations, respectively, as depicted in Figure 1.

For metal−salen^A complexes that contain neither d^0 metal ion nor bidentate co-ligand, a question is whether the species with a nonplanar salen^A can in some cases prevail and play an important role in related catalytic processes. It was proposed that nonplanar salen^A ligands exist in [Ru^{II}(salen^A)(NO)(L)]$^+$ (L = MeCN, thiiranes)[3] and [Ru^{II}(salen^A)(CO)$_2$],[4] the structures of which, however, have not been confirmed by X-ray crystal analysis. Recent DFT calculations on Mn−salen^A-catalyzed alkene oxidation[5] by Morokuma and co-workers revealed stable intermediates *cis*(*O*,*N*)-*β*-[Mn^{V}O(salen^A)(OAc)] and *cis*(*N*,*O*)-*β*-[Mn^{V}O(salen^A)(OAc)], albeit with a stability lower than the intermediate *trans*-[Mn^{V}O(salen^A)(OAc)] bearing the salen^A ligand in a planar coordination mode.[5a]

In a previous work,[6] we reported the asymmetric intramolecular cyclopropanation of *cis*-alkenes catalyzed by [Ru^{II}(salen^A)(PPh$_3$)$_2$] and [Ru^{II}(salen^A)(CO)], along with the X-ray crystal structures of such catalysts and related ruthenium−carbene complexes [Ru^{II}(salen^A)(CAr$_2$)(L)] (L = pyridine or *N*-methylimidazole). The salen^A ligands in these crystal structures[6] and in all the other crystal structures of ruthenium−salen^A complexes reported in the literature[4b,7] exclusively adopt a planar coordination mode.

Upon further studies on ruthenium−salen^A complexes, we obtained and structurally characterized several *cis*-*β*-[Ru(salen^A)(CO)$_2$] complexes (**1a**–**c**, Scheme 1) in which the salen^A ligands unusually adopt a nonplanar coordination mode (Scheme 1). Herein we report the isolation and X-ray crystal structures of complexes **1** (**1** = **1a**–**c**) and their catalytic properties toward asymmetric intramolecular cyclopropanation of *trans*-alkenes under light irradiation as well as in the dark. DFT calculations on the possible intermediates in the **1**-catalyzed asymmetric cyclopropanation reactions are also reported here, revealing that *the intramolecular cyclopropanation of the cis-β-ruthenium−carbene complex is the most favorable pathway*. The salen^A ligand primarily employed in this work is Jacobsen's salen ligand (salen^{A1}, Scheme 1).[1] Metallosalen catalysts containing Jacobsen' salen ligand have important applications in a number of highly enantioselective organic transformations.[1]

Results

Synthesis. Reactions of Ru$_3$(CO)$_{12}$ with enantiopure (1*R*,2*R*)-H$_2$salen^A in 1,2,4-trichlorobenzene (1,2,4-TCB) at ∼190 °C under argon in the dark for 6 h afforded chiral complexes *cis*-*β*-[Ru^{II}(salen^A)(CO)$_2$] (salen^A = salen^{A1}, **1a**; salen^{A2}, **1b**; salen^{A3}, **1c**), as depicted in reaction 1 of Scheme 1. This synthetic route to [Ru^{II}(salen^A)(CO)$_2$] is different from previously reported ones involving the reaction of {[Ru(CO)$_2$Cl$_2$]}$_n$ with Na$_2$(salen^A).[4] We have tried to extend reaction 1 to the unsubstituted salen

(3) Sauve, A. A.; Groves, J. T. *J. Am. Chem. Soc.* **2002**, *124*, 4770.
(4) (a) Thornback, J. R.; Wilkinson, G. *J. Chem. Soc., Dalton Trans.* **1978**, 110. (b) Leung, W. H.; Chan, E. Y. Y.; Chow, E. K. F.; Williams, I. D.; Peng, S. M. *J. Chem. Soc., Dalton Trans.* **1996**, 1229.
(5) (a) Khavrutskii, I. V.; Musaev, D. G.; Morokuma, K. *J. Am. Chem. Soc.* **2003**, *125*, 13879. (b) Khavrutskii, I. V.; Musaev, D. G.; Morokuma, K. *Proc. Natl. Acad. Sci. U.S.A.* **2004**, *101*, 5743.
(6) Li, G.-Y.; Zhang, J.; Chan, P. W. H.; Xu, Z.-J.; Zhu, N.; Che, C.-M. *Organometallics* **2006**, *25*, 1676.
(7) (a) Odenkirk, W.; Rheingold, A. L.; Bosnich, B. *J. Am. Chem. Soc.* **1992**, *114*, 6392. (b) Nakajima, K.; Ando, Y.; Mano, H.; Kojima, M. *Inorg. Chim. Acta* **1998**, *274*, 184. (c) Takeda, T.; Irie, R.; Katsuki, T. *Synlett* **1999**, 1166. (d) Works, C. F.; Jocher, C. J.; Bart, G. D.; Bu, X.; Ford, P. C. *Inorg. Chem.* **2002**, *41*, 3728. (e) Bordini, J.; Hughes, D. L.; Da Motta Neto, J. D.; da Cunha, C. J. *Inorg. Chem.* **2002**, *41*, 5410. (f) Miller, J. A.; Hennessy, E. J.; Marshall, W. J.; Scialdone, M. A.; Nguyen, S. T. *J. Org. Chem.* **2003**, *68*, 7884. (g) Man, W.-L.; Tang, T.-M.; Wong, T.-W.; Lau, T.-C.; Peng, S.-M.; Wong, W.-T. *J. Am. Chem. Soc.* **2004**, *126*, 478. (h) Man, W.-L.; Lam, W. W. Y.; Yiu, S.-M.; Lau, T.-C.; Peng, S.-M. *J. Am. Chem. Soc.* **2004**, *126*, 15336. (i) Yeung, W.-F.; Lau, P.-H.; Lau, T.-C.; Wei, H.-Y.; Sun, H.-L.; Gao, S.; Chen, Z.-D.; Wong, W.-T. *Inorg. Chem.* **2005**, *44*, 6579. (j) Wong, C.-Y.; Man, W.-L.; Wang, C.; Kwong, H.-L.; Wong, W.-Y.; Lau, T.-C. *Organometallics* **2008**, *27*, 324. (k) Man, W.-L.; Kwong, H.-K.; Lam, W. W. Y.; Xiang, J.; Wong, T.-W.; Lam, W.-H.; Wong, W.-T.; Peng, S.-M.; Lau, T.-C. *Inorg. Chem.* **2008**, *47*, 5936.

Scheme 1

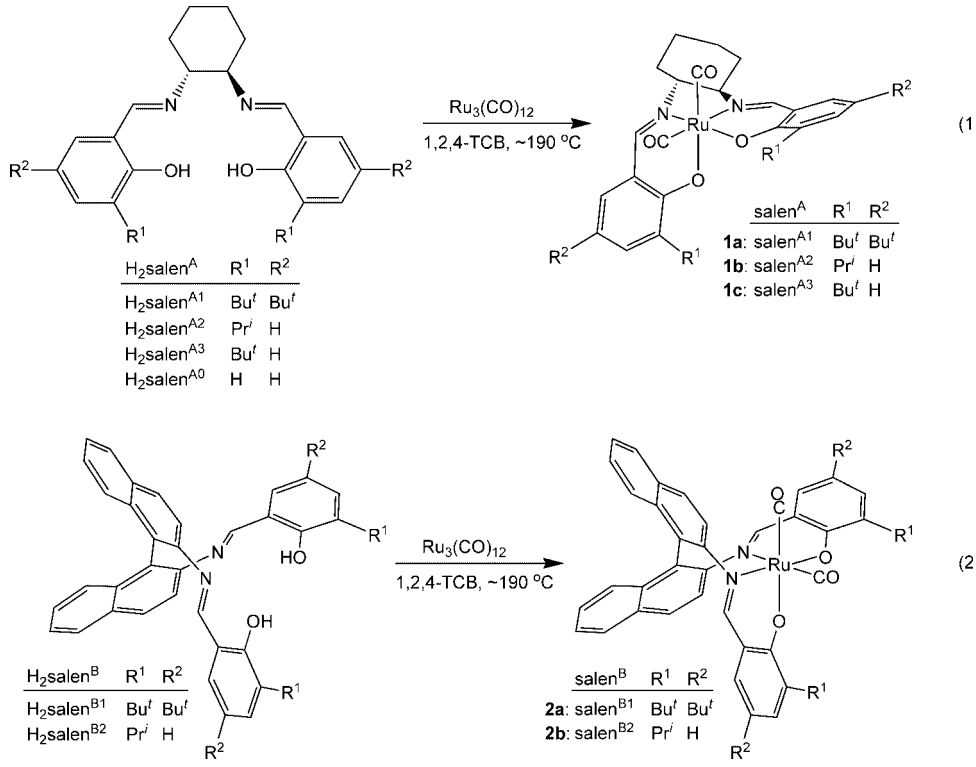

ligand, H_2salen^{A0} (Scheme 1), but no $[Ru^{II}(salen^{A0})(CO)_2]$ was detected or isolated from the reaction mixture, suggesting that the bulky R^1 substituents Bu^t or Pr^i in $salen^A$ contribute significantly to the formation of these bis(carbonyl) complexes in the reaction.

To compare the coordination behavior of $salen^{A1}$−$salen^{A3}$ in **1** with that of binaphthyl-containing $salen^B$ ligands, the latter usually adopting a nonplanar coordination mode in their complexes with transition metal ions[2d] as described above, we treated $Ru_3(CO)_{12}$ with racemic H_2salen^{B1} and H_2salen^{B2} (Scheme 1) under the conditions similar to those for reaction 1 and isolated *cis*-β-$[Ru^{II}(salen^B)(CO)_2]$ ($salen^B$ = $salen^{B1}$, **2a**; $salen^{B2}$, **2b**) (reaction 2 in Scheme 1).

Complexes **1a**−**c** and **2a**,**b** are stable when kept away from light. Under dark conditions, neither isomerization to *trans* counterparts nor decomposition to mono(carbonyl) analogues was observed for their solutions in $CHCl_3$ upon standing at room temperature for a week or upon heating to 55 °C for ~30 min.

Spectral Features. The ^1H NMR spectra of **1a**−**c** in $CDCl_3$ show well-resolved signals (see, for example, Figure 2). A notable feature in these spectra is the large splitting between the N=C−*H* signals (H^a and $H^{a'}$, Figure 2) of $salen^A$, with $\Delta\delta$ being 0.31 (**1a**), 0.30 (**1b**), and 0.33 (**1c**) ppm. Such a splitting for the nonplanar $salen^{A1}$ in **1a** is significantly larger than that ($\Delta\delta$ 0.08 ppm) for planar $salen^{A1}$ in structurally characterized *trans*-$[Ru^{II}(salen^{A1})(NO)(Cl)]$.[4b] As only a single set of the $salen^A$ signals appears in the spectra, and no apprecable changes in the spectra were observed upon increasing the temperature from 25 to 55 °C, there should be no significant dissociation of **1a**−**c** into their mono(carbonyl) analogues in the solutions on the ^1H NMR time scale.

For **2a**,**b**, their ^1H NMR spectra show the H^a, $H^{a'}$ signals at δ 8.13, 7.56 ppm for **2a** and 8.15, 7.56 ppm for **2b**, with a splitting ($\Delta\delta$ 0.57 (**2a**), 0.59 (**2b**) ppm) larger than that for **1a**−**c**.

The IR spectra of **1a**−**c** exhibit two intense ν(CO) bands at ~2040 and ~1965 cm^{-1}, which compare well with the ν(CO) bands for **2a**,**b** (~2045, ~1975 cm^{-1}).[8] In the FAB mass spectra, prominent cluster peaks ascribable to the parent ions of **1a**−**c** and **2a**,**b** were found.

X-ray Crystal Structures. Diffraction-quality crystals **1a**·3MeOH, **1c**, and **2a**·0.5CH_2Cl_2 were obtained. Their structures determined by X-ray crystallography all feature a *cis*-β configuration and are depicted in Figures 3 and 4. Listed in Table 1 are the crystal data and structural refinement data for these complexes. The crystal **2a**·0.5CH_2Cl_2 is racemic, and there are two independent molecules (a pair of Δ and Λ enantiomers) in the asymmetric unit. Both crystals **1a**·3MeOH and **1c** are chiral, as confirmed by the respective Flack parameters of 0.02(5) and −0.01(3).

In the structures of **1a** and **1c**, the Ru−N and Ru−O distances fall within the ranges of 2.028(7)−2.071(3) and 2.044(5)−2.094(6) Å, respectively, which are comparable to those in **2a** (Ru−N 2.045(4)−2.090(4) Å, Ru−O 2.049(3)−2.058(4) Å). The two phenyl planes of the $salen^A$ ligand form a dihedral angle of 52.5(3)° in **1a** and 53.3(1)° in **1c**, close to the corresponding angle of 58.9(2)° (mean) in **2a**.

The two *cis*-carbonyl groups in each of the complexes make a similar C−Ru−C angle of 89.3(5)° for **1a**, 90.46(15)° for **1c**, and 91.4(3)° (mean) for **2a**. In all the three complexes, the Ru−C(CO) distance for the CO group *trans* to the O atom of the salen ligand (**1a**, 1.869(11) Å; **1c**, 1.855(4) Å; **2a**, 1.837(26) Å (mean)) is shorter than that *trans* to the N atom of the salen ligand (**1a**, 1.878(12) Å; **1c**, 1.908(4) Å; **2a**, 1.917(31) Å (mean)).

(8) Note that the ν(CO) bands of **1a** are significantly different from those (1890 and 1920 cm^{-1}) of the *cis*-$[Ru^{II}(salen^{A1})(CO)_2]$ prepared from the reaction of Na_2salen^{A1} with $[\{Ru(CO)_2Cl_2\}_n]$ in THF.[4b]

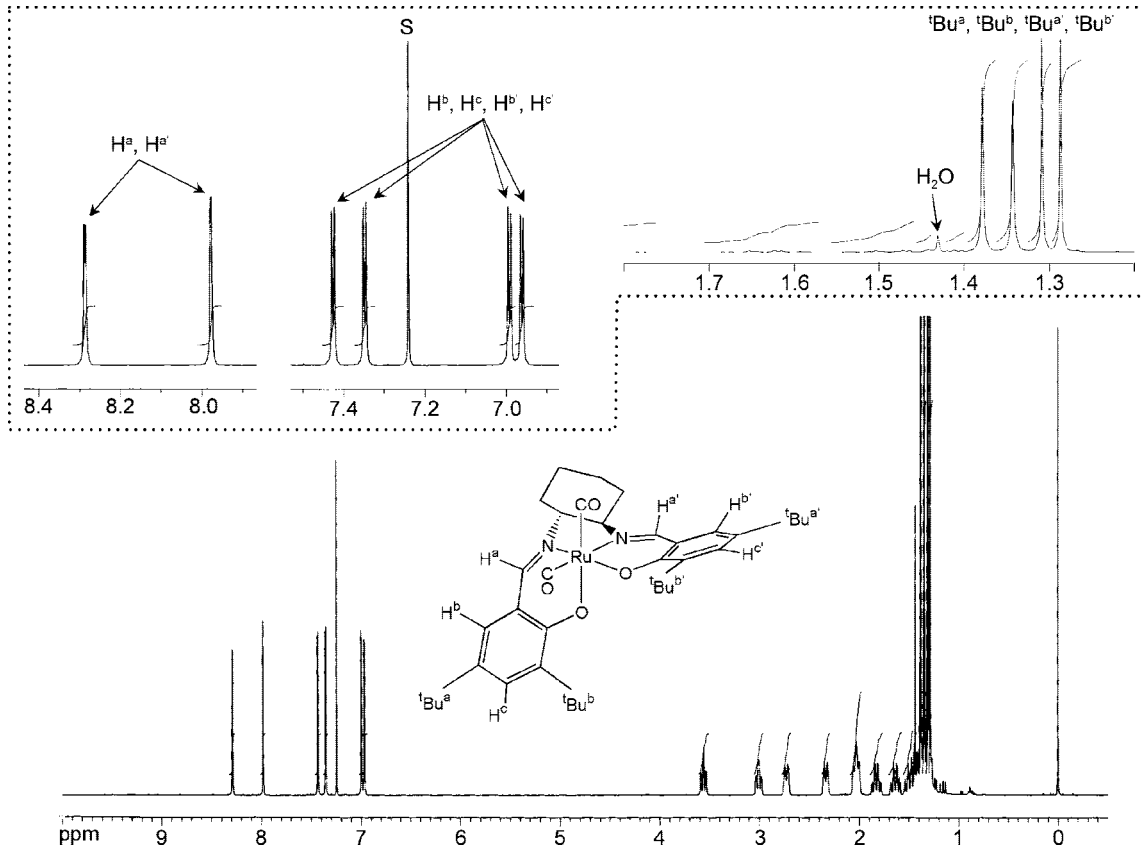

Figure 2. ^{1}H NMR spectrum (400 MHz) of **1a** in $CDCl_3$. On the top is a clearer view of the N=C−H (H^a, $H^{a'}$) and $C_6H_2Bu^t_2$ signals.

Asymmetric Intramolecular Cyclopropanation. We found that complexes **1a**−**c** can catalyze asymmetric intramolecular cyclopropanation of *trans*-allylic diazoacetates. The catalytic reactions were initially performed by slow addition of the substrates to minimize byproducts such as carbene dimers.[9] Examination of the effects of solvent and catalyst on the intramolecular cyclopropanation of **3a** revealed that CH_2Cl_2 with 0.03% (v/v) MeOH is the solvent of choice (Table S1 in Supporting Information) and **1a** is a better catalyst than **1b**,**c** and **2a**,**b** (Table S2 in Supporting Information). Addition of **3a** to a CH_2Cl_2 solution with 0.03% MeOH in the presence of 1 mol % of **1a** over 6 h followed by refluxing the mixture for an additional 10 h afforded **4a** in 92% yield and 96% ee (entry 1, Table S2 in Supporting Information). By employing 0.5 mol % of **1a**, the reaction gave **4a** in 91% yield (182 turnovers) and 97% ee within 30 h. For substrates **3b**−**g** (CH_2Cl_2, 0.03% MeOH, 1 mol % of **1a**), the reactions gave **4b**−**g** in 56−95% yields and 50−81% ee (18 h, Table S2 in Supporting Information).

Further studies revealed the following features: (i) the yield and ee of **4a** were virtually unaffected by rapid addition of substrate **3a**, regardless of whether MeOH was present or not; (ii) irradiation of the reaction mixture with an incandescent lamp shortened the reaction time from ∼18 to 3 h, with **4a** obtained in 89% yield and 90% ee in the absence of MeOH; (iii) introducing 0.03−0.17% MeOH additive resulted in the isolation of **4a** in 90−91% yields and 95−98% ee (Table 2 and Table S3 in Supporting Information) from the reaction with irradiation by light; (iv) minor variations of the product yields (85−91%) and ee (84−90%) were encountered among the solvent additives EtOH, THF, and CH_3CN (0.03% v/v) (Table S4 in Supporting Information) with MeOH additive giving the optimal result.

Irradiation of a solution of **1a** in CH_2Cl_2 with an incandescent lamp for 2 h resulted in a decrease in the amount of **1a**, accompanied by appearance of a new species featuring a single ν(CO) band at 1915 cm^{-1} (see the IR spectrum in Figure S1 in Supporting Information)[10] similar to those (1915−1939 cm^{-1}) reported for [Ru^{II}(salen^A)(CO)].[6] Subsequent addition of methanol (0.03%) and **3a** (0.25 mmol) to the irradiated solution followed by refluxing the mixture for 7 h under dark condition afforded **4a** in 90% yield and 91% ee.

When the cyclopropanation reactions were performed by directly dissolving a mixture of **3b**−**g** and 1 mol % of **1a** in CH_2Cl_2 with 0.03% MeOH under light irradiation, **4b**−**g** were obtained in 75−96% yields and 58−95% ee within 3−5 h, as shown in Table 2. Under the same conditions, the reaction for **3h**, an ineffective substrate under no light irradiation, gave **4h** in 77% yield and 58% ee. *cis*-Allylic diazoacetate **3i** was an inferior substrate for the reaction; its conversion to **4i** catalyzed by **1a** had a yield of 48% with 51% ee.

DFT Calculations. As metal-catalyzed cyclopropanations of diazo compounds are widely presumed to occur via metal−carbene intermediates,[11] we performed DFT calculations on the

(9) (a) Doyle, M. P.; Pieters, R. J.; Martin, S. F.; Austin, R. E.; Oalmann, C. J.; Müller, P. *J. Am. Chem. Soc.* **1991**, *113*, 1423. (b) Doyle, M. P.; Austin, R. E.; Bailey, A. S.; Dwyer, M. P.; Dyatkin, A. B.; Kalinin, A. V.; Kwan, M. M. Y.; Liras, S.; Oalmann, C. J.; Pieters, R. J.; Protopopova, M. N.; Raab, C. E.; Roos, G. H. P.; Zhou, Q.-L.; Martin, S. F. *J. Am. Chem. Soc.* **1995**, *117*, 5763.

(10) The UV−visible spectral changes of **1a** upon light irradiation revealed blurred isosbestic points (Figure S2 in Supporting Information), presumably owing to secondary reaction(s) after formation of [Ru^{II}(salen^{A1})(CO)].

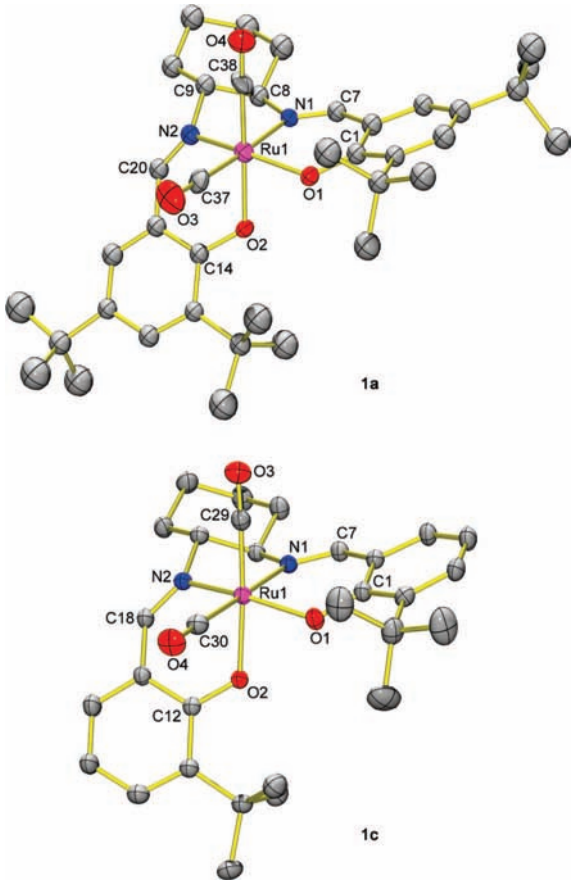

Figure 3. Structures of **1a** and **1c** with omission of hydrogen atoms (thermal ellipsoid probability: 30%).

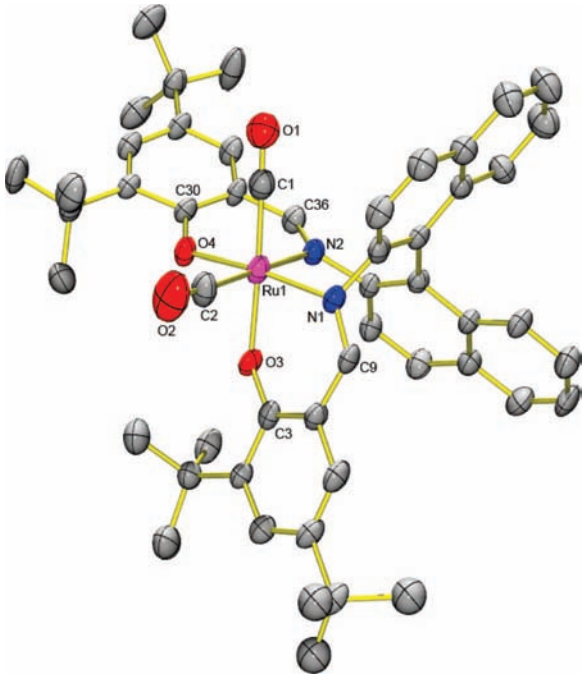

Figure 4. Structure of **2a** with omission of hydrogen atoms (thermal ellipsoid probability: 30%). Note that there are a pair of Δ and Λ enantiomers in the asymmetric unit (only the Λ enantiomer is shown).

ruthenium−carbene intermediates possibly involved in the intramolecular cyclopropanation of **3a** mediated by model complex *cis-β*-[Ru^{II}($salen^{A0}$)$(CO)_2$] with the same chirality as that of **1a**. These intermediates include *cis-β* species **RC-O** and **RC-N** and *trans* species **RC-CO** and **RC-H_2O** (Chart 1; here H_2O was employed as a model for the coordinating solvent molecules in the catalytic system). The two *cis-β* species could be formed from the reaction of **3a** with *cis-β*-[Ru^{II}($salen^{A0}$)$(CO)_2$] or with the *cis-β*-mono(carbonyl) species generated upon light irradiation (note the behavior of **1a** toward light irradiation described above), whereas the two *trans* species could be produced by, for example, *cis-trans* isomerization from **RC-O** or **RC-N** and/or solvent substitution for the CO group.

Figure 5 shows the calculated structures of **RC-O**, **RC-N**, **RC-CO**, and **RC-H_2O**, which have Ru−C(carbene) distances of 1.853−1.898 Å. Reactions of the four species to afford the enantiomers of the intramolecular cyclopropanation products, **PR1** and **PR2**, via transition states **TS1** and **TS2**, respectively, are depicted in Figure 6. The calculated relative energies (ΔE) and free energies (ΔG) of these ruthenium−carbene complexes, the corresponding transition states, and the cyclopropanation products are listed in Table 3. Figure 7 shows the free energy profiles for the cyclopropanation reactions based on **RC-O**, **RC-N**, **RC-CO**, and **RC-H_2O**. The potential energy profiles for **TS1-O** and **TS2-O** along the reaction coordinate (SI) are shown in Figure S4 in Supporting Information.

Discussion

Ruthenium−$salen^A$ complexes have received considerable attention owing to their catalytic efficiency for C−O, C−C, C−N, and N−S bond formation reactions.[1g,h,m,12] In 1989, we reported that *trans*-[Ru^{III}($salen^A$)(PPh_3)(py)]$^+$ and *trans*-[Ru^{III}($salen^A$)(PPh_3)(X)] (X = N_3^-, TsO^-) can catalyze epoxidation of alkenes.[13] Since then, a variety of organic transformations catalyzed by ruthenium−$salen^A$ complexes have been reported, mainly by the groups of Bosnich,[7a,14] Katsuki,[15−22] Groves,[3] Nguyen,[23] and our group;[6,24] the ruthenium−$salen^A$ catalysts employed in these reactions include the followings:

(11) Selected reviews: (a) Doyle, M. P. In *Comprehensive Organometallic Chemistry II*; Hegedus, L. S., Ed.; Pergamon: Oxford, 1995; Vol. 12, p 387. (b) Doyle, M. P.; Forbes, D. C. *Chem. Rev.* **1998**, *98*, 911. (c) Doyle, M. P.; McKervey, M. A.; Ye, T. *Modern Catalytic Methods for Organic Synthesis with Diazo Compounds*; Wiley: New York, 1998.

(12) For reviews on organic transformations catalyzed by ruthenium complexes including ruthenium−$salen^A$ catalysts, see: (a) Bosnich, B. *Aldrichimica Acta* **1998**, *31*, 76. (b) Trost, B. M.; Toste, F. D.; Pinkerton, A. B. *Chem. Rev.* **2001**, *101*, 2067. (c) Nishiyama, H. *Top. Organomet. Chem.* **2004**, *11*, 81. (d) Yamamoto, Y.; Itoh, K. *Top. Organomet. Chem.* **2004**, *11*, 249. (e) Arends, I. W. C. E.; Kodama, T.; Sheldon, R. A. *Top. Organomet. Chem.* **2004**, *11*, 277. (f) *Ruthenium in Organic Synthesis*; Murahashi, S.-I., Ed.; Wiley-VCH: Weinheim, Germany, 2004. (g) Irie, R.; Katsuki, T. *Chem. Rec.* **2004**, *4*, 96. (h) Chatterjee, D. *Coord. Chem. Rev.* **2008**, *252*, 176.

(13) Leung, W.-H.; Che, C.-M. *Inorg. Chem.* **1989**, *28*, 4619.

(14) (a) Odenkirk, W.; Whelan, J.; Bosnich, B. *Tetrahedron Lett.* **1992**, *33*, 5729. (b) Ellis, W. W.; Odenkirk, W.; Bosnich, B. *Chem. Commun.* **1998**, 1311.

(15) (a) Takeda, T.; Irie, R.; Shinoda, Y.; Katsuki, T. *Synlett* **1999**, 1157. (b) Nakata, K.; Takeda, T.; Mihara, J.; Hamada, T.; Irie, R.; Katsuki, T. *Chem.−Eur. J.* **2001**, *7*, 3776.

(16) Mihara, J.; Hamada, T.; Takeda, T.; Irie, R.; Katsuki, T. *Synlett* **1999**, 1160.

(17) (a) Uchida, T.; Irie, R.; Katsuki, T. *Synlett* **1999**, 1163. (b) Uchida, T.; Irie, R.; Katsuki, T. *Synlett* **1999**, 1793. (c) Uchida, T.; Irie, R.; Katsuki, T. *Tetrahedron* **2000**, *56*, 3501. (d) Uchida, T.; Katsuki, T. *Synthesis* **2006**, 1715.

(18) (a) Saha, B.; Uchida, T.; Katsuki, T. *Synlett* **2001**, 114. (b) Uchida, T.; Saha, B.; Katsuki, T. *Tetrahedron Lett.* **2001**, *42*, 2521. (c) Saha, B.; Uchida, T.; Katsuki, T. *Tetrahedron: Asymmetry* **2003**, *14*, 823.

(19) (a) Masutani, K.; Uchida, T.; Irie, R.; Katsuki, T. *Tetrahedron Lett.* **2000**, *41*, 5119. (b) Miyata, A.; Murakami, M.; Irie, R.; Katsuki, T. *Tetrahedron Lett.* **2001**, *42*, 7067.

Table 1. Crystal Data and Structural Refinement for **1a**·3MeOH, **1c**, and **2a**·0.5CH_2Cl_2

	1a·3MeOH	**1c**	**2a**·0.5CH_2Cl_2
formula	$C_{41}H_{64}N_2O_7Ru$	$C_{30}H_{36}N_2O_4Ru$	$C_{52.50}H_{55}ClN_2O_4Ru$
M_r	798.01	589.68	914.51
crystal system	monoclinic	orthorhombic	triclinic
space group	$P2_1$	$P2_1\ 2_1\ 2_1$	$P\bar{1}$
a, Å	9.439(2)	11.893(2)	15.678(3)
b, Å	17.257(4)	12.535(3)	16.111(3)
c, Å	13.365(3)	19.076(4)	20.109(4)
α, deg	90.00	90.00	85.14(3)
β, deg	93.96(3)	90.00	88.56(3)
γ, deg	90.00	90.00	68.73(3)
F(000)	848	1224	1908
V, Å^3	2171.8(8)	2843.8(10)	4716.2(16)
Z	2	4	4
ρ_{calc}, g cm^{-3}	1.220	1.377	1.288
μ(Mo Kα), mm^{-1}	0.407	0.587	0.435
$2\theta_{max}$, deg	47.96	51.24	50.34
reflections collected	6201	20995	21678
independent reflections	3728	5287	11032
parameters	262	334	1084
final R indices ($I > 2\sigma(I)$)	$R1 = 0.050$ $wR2 = 0.112$	$R1 = 0.026$ $wR2 = 0.077$	$R1 = 0.042$ $wR2 = 0.093$
goodness-of-fit	0.82	1.17	0.76
largest diff. peak/hole, e Å^{-3}	0.32/−0.33	0.34/−0.54	0.42/−0.37
Flack parameter	0.02(5)	−0.01(3)	

(i) *trans*-[Ru^{II}($salen^A$)(NO)(H_2O)]SbF_6 for Diels−Alder reaction,[7a] Mukaiyama reaction,[14a] inter- and intramolecular ene reaction,[14b] and conversion of thiiranes to trithiolanes and tetrathianes;[3] (ii) *trans*-[Ru^{II}($salen^A$)(NO)Cl] for asymmetric epoxidation of alkenes,[15] hetero-Diels−Alder reaction and kinetic resolution of racemic epoxides,[16] inter-[17] and intramolecular[18a,c] cyclopropanation of alkenes, and aerobic oxidation of alcohols;[19] (iii) [Ru^{II}($salen^A$)(CO)] for asymmetric sulfimidation[20] and intramolecular cyclopropanation[6] and intermolecular aziridination of alkenes;[21] (iv) *trans*-[Ru^{II}($salen^A$)(NO)(X)] (X = Cl, OH) for aerobic oxidative desymmetrization of *meso*-diols;[22] (v) *trans*-[Ru^{II}($salen^A$)(PPh_3)$_2$] for oxidation of alcohols[25] and hydroxamic acid,[26a] Diels−Alder reaction,[26b] asymmetric inter-[23b] and intramolecular cyclopropanation of alkenes,[6] amidation of silyl enol ethers and cholesteryl acetates, and aziridination of alkenes;[24] (vi) *trans*-[Ru^{II}($salen^A$)(py)$_2$] for asymmetric intermolecular cyclopropanation of alkenes;[7f,23] (vii) *trans*-[Ru^{II}($salen^A$)(CO)(PPh_3)] for oxidation of alcohols.[27] All these ruthenium catalysts were reported to contain $salen^A$ ligands in a planar coordination mode.

In the presence of β-hydroxy ketone or 1,3-diketone, the aerobic oxidative resolution of racemic alcohols catalyzed by *trans*-[Ru^{II}($salen^A$)(NO)Cl] probably involves *cis*-β-Ru^{II}−$salen^A$ intermediates bearing a bidentate β-hydroxy ketone or 1,3-diketone co-ligand, as proposed by Katsuki and co-workers.[22c] Groves and co-workers proposed that, in the *trans*-[Ru^{II}($salen^A$)(NO)(H_2O)]SbF_6-catalyzed conversion of thiiranes to trithiolanes and tetrathianes, the catalyst initially reacts with thiirane to generate *cis*-β-[Ru^{II}($salen^A$)(NO)(thiirane)]SbF_6 intermediates, which contain monodentate NO and thiirane ligands and are formulated on the basis of ^{1}H NMR measurements.[3]

Catalysts **1a**,**c** are, to the best of our knowledge, the first examples of structurally characterized metal−$salen^A$ complexes that contain neither d^0 metal ion nor bidentate co-ligand but bear $salen^A$ ligand in a nonplanar coordination mode. The *cis*-β configuration of **1a**,**c** is not a favored one for a Ru^{II}−$salen^{A1}$ complex,[4b,6,7] unlike that of structurally characterized **2a**, which contains the $salen^{B1}$ ligand intrinsically favoring such a configuration.[2d] Recently, Katsuki and co-workers reported the X-ray crystal structures of two *cis*-β-[Ru^{II}(salalen)($CO)_2$] complexes;[28] the salalen ligands, a hybrid of salen with salan (tetrahydro salen) ligands, also intrinsically favor a nonplanar coordination.[29] For example, the crystal structure of [Al^{III}(salalen)Cl][30a] has a distorted trigonal pyramidal coordination geometry similar to that of [Al^{III}($salen^{B1}$)Cl],[30b] but different from the square pyramidal geometry in [Al^{III}($salen^{A1}$)X] (X = OAc, OR).[30c] A comparison between the structures of **1a** and *cis*-β-[Ru^{II}(salalen)($CO)_2$][28] is shown in Figure S5 in Supporting Information.

In contrast to the poor catalytic activity of **1a** for asymmetric sulfimidation,[28] **1a**−**c** are highly selective catalysts for asymmetric intramolecular cyclopropanation of *trans*-allylic diazoacetates, as shown from the high yields (83−91%) and excellent ee (90−98%) obtained for **4a**−**d** (entries 1−6 in Table 2). For the conversion of *cis*-allylic diazoacetate **3i** to **4i**, the ee value (51%) in the **1a**-catalyzed reaction is substantially lower than the 90% ee in the same reaction catalyzed by *trans*-[Ru^{II}($salen^A$)(PPh_3)$_2$].[6] As the intramolecular cyclopropanation catalyzed by **1a**−**c** proceeded more rapidly under light irradia-

(20) (a) Murakami, M.; Uchida, T.; Katsuki, T. *Tetrahedron Lett.* **2001**, *42*, 7071. (b) Tamura, Y.; Uchida, T.; Katsuki, T. *Tetrahedron Lett.* **2003**, *44*, 3301.

(21) Omura, K.; Murakami, M.; Uchida, T.; Irie, R.; Katsuki, T. *Chem. Lett.* **2003**, *32*, 354.

(22) (a) Shimizu, H.; Katsuki, T. *Chem. Lett.* **2003**, *32*, 480. (b) Shimizu, H.; Onitsuka, S.; Egami, H.; Katsuki, T. *J. Am. Chem. Soc.* **2005**, *127*, 5396. (c) Nakamura, Y.; Egami, H.; Matsumoto, K.; Uchida, T.; Katsuki, T. *Tetrahedron* **2007**, *63*, 6383.

(23) (a) Miller, J. A.; Jin, W.; Nguyen, S. T. *Angew. Chem., Int. Ed.* **2002**, *41*, 2953. (b) Miller, J. A.; Gross, B. A.; Zhuravel, M. A.; Jin, W.; Nguyen, S. T. *Angew. Chem., Int. Ed.* **2005**, *44*, 3885.

(24) Liang, J.-L.; Yu, X.-Q.; Che, C.-M. *Chem. Commun.* **2002**, 124.

(25) Bhowon, M. G.; Wah, H. L. K.; Narain, R. *Polyhedron* **1999**, *18*, 341.

(26) (a) Flower, K. R.; Lightfoot, A. P.; Wan, H.; Whiting, A. *J. Chem. Soc., Perkin Trans. 1* **2002**, 2058. (b) Howard, J. A. K.; Ilyashenko, G.; Sparkes, H. A.; Whiting, A. *Dalton Trans.* **2007**, 2108.

(27) Kumar, K. N.; Ramesh, R. *Polyhedron* **2005**, *24*, 1885.

(28) Fujita, H.; Uchida, T.; Irie, R.; Katsuki, T. *Chem. Lett.* **2007**, *36*, 1092.

(29) Yeori, A.; Gendler, S.; Groysman, S.; Goldberg, I.; Kol, M. *Inorg. Chem. Commun.* **2004**, *7*, 280.

(30) (a) Saito, B.; Egami, H.; Katsuki, T. *J. Am. Chem. Soc.* **2007**, *129*, 1978. (b) Evans, D. A.; Janey, J. M.; Magomedov, N.; Tedrow, J. S. *Angew. Chem., Int. Ed.* **2001**, *40*, 1884. (c) Chen, P.; Chisholm, M. H.; Gallucci, J. C.; Zhang, X.; Zhou, Z. *Inorg. Chem.* **2005**, *44*, 2588.

Table 2. Intramolecular Cyclopropanation of Allylic Diazoacetates Catalyzed by *cis*-β-[Ru^{II}(salen^{A})(CO)$_2$] (**1a**−**c**)[a]

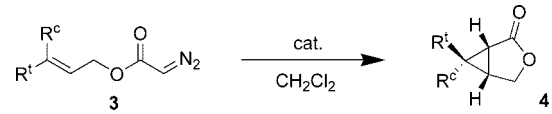

3 **4**

entry	substrate	product	catalyst	yield[b] (%)	ee (%)
1	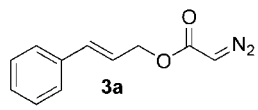 **3a**	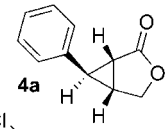 **4a**	**1a**	91	98
2			**1b**	83	95
3			**1c**	85	90
4	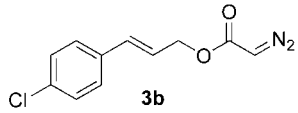 **3b**	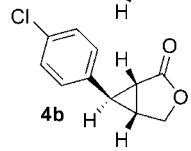 **4b**	**1a**	88	90
5	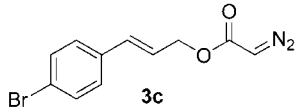 **3c**	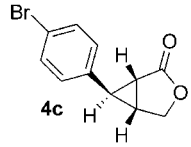 **4c**	**1a**	87	94
6	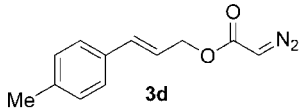 **3d**	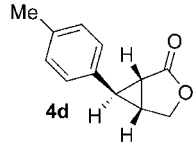 **4d**	**1a**	84	95
7	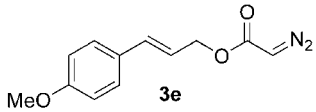 **3e**	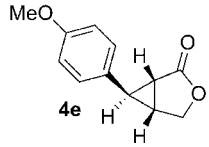 **4e**	**1a**	96	77
8	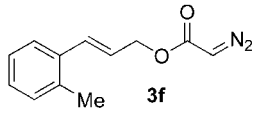 **3f**	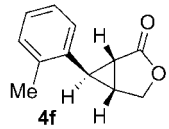 **4f**	**1a**	75	79
9	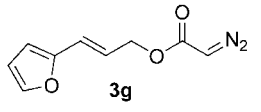 **3g**	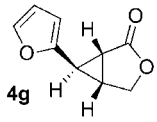 **4g**	**1a**	88	58
10	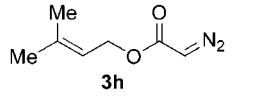 **3h**	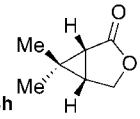 **4h**	**1a**	77	58
11[c]	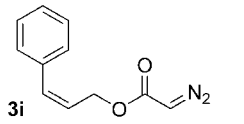 **3i**	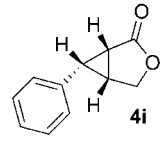 **4i**	**1a**	48	51

[a] Reaction conditions: 0.25 mmol **3**, 1 mol % of **1**, 3 mL of CH_2Cl_2 with 0.03% v/v MeOH, refluxing for 3−5 h under argon and irradiation with an incandescent lamp (300 W). [b] Isolated yield. [c] Refluxing for 24 h.

tion, we suggest that the light irradiation resulted in decarbonylation of **1** to give more reactive mono(carbonyl) species, and this has been supported by the results of monitoring the photochemical reaction of **1a** in CH_2Cl_2 solution, as described in the previous section.

Highly enantioselective metal-catalyzed asymmetric intramolecular cyclopropanation of allylic diazoacetates[31] was first reported by Doyle and co-workers using catalysts [Rh$_2$(5*S*-MEPY)$_4$] and [Rh$_2$(5*S*-MEPY)$_4$] (MEPY = methyl 2-pyrrolidone-5-carboxylate).[9] These Rh-catalyzed reactions show ≥94% ee for *cis*-allylic diazoacetates, with lower ee values of 54−85% obtained for *trans*-allylic diazoacetates including **3a**.[9]

(31) For reviews including transition-metal-catalyzed asymmetric intramolecular cyclopropanation, see: (a) Ref 11. (b) Doyle, M. P.; Hu, W. *Synlett* **2001**, 1364. (c) Lebel, H.; Marcoux, J.-F.; Molinaro, C.; Charette, A. B. *Chem. Rev.* **2003**, *103*, 977. (d) Doyle, M. P. *Top. Organomet. Chem.* **2004**, *13*, 203. (e) Doyle, M. P. In *Modern Rhodium-Catalyzed Organic Reactions*; Evans, P. A., Ed.; Wiley-VCH: Weinheim, Germany, 2005; p 341.

Chart 1

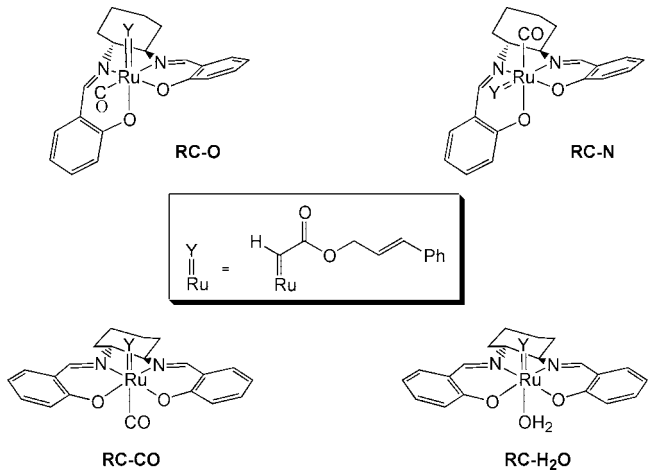

In the conversion of **3a** to **4a** catalyzed by $[Rh_2(4S\text{-MPPIM})_4]$ (4*S*-MPPIM = methyl 1-(3-phenylpropanoyl)imidazolidin-2-one-4(*S*)-carboxylate), Doyle and co-workers obtained **4a** with 96% ee albeit in 61% yield.[32] Nishiyama and co-workers reported that *trans*-$[RuCl_2(4\text{-X-pybox})(C_2H_4)]$ (X = Me_2N, MeO, H, Cl, MeO_2C; pybox = bis(oxazolinyl)pyridine) catalyzes the same reaction to give **4a** in 67−83% yields and 52−89% ee.[33] Besides the rhodium catalyst and ruthenium−pybox catalysts, ruthenium porphyrin $[Ru^{II}(D_4\text{-Por*})(CO)(MeOH)]$ (D_4-Por* = *meso*-tetrakis-{(1*S*,4*R*,5*R*,8*S*)-1,2,3,4,5,6,7,8-octahydro-1,4:5,8-dimethano-anthracen-9-yl}porphyrinatodianion) was found, in our previous work, to catalyze the cyclopropanation of **3a** to give **4a** in 85% ee and 60% yield.[34] Katsuki and co-workers reported an up to 97% ee albeit ≤75% yields for the conversion of **3a** to **4a** catalyzed by $[Co^{II}(salen^A)]$.[17d,18b,c] In contrast to these rhodium-, ruthenium-, and cobalt-catalyzed reactions, the **1a**-catalyzed reaction of **3a** afforded **4a** in both an excellent yield (91%) and an excellent ee (98%).

Compared with **1a**, *trans*-$[Ru^{II}(salen^A)(PPh_3)_2]$ ($salen^A$ = $salen^{A0}$, $salen^{A4}$−$salen^{A8}$) and $[Ru^{II}(salen^A)(CO)]$ ($salen^A$ = $salen^{A4}$, $salen^{A6}$, $salen^{A7}$) bearing $salen^A$ ligands in a planar configuration are less efficient catalysts for the intramolecular cyclopropanation of **3a**, with **4a** obtained in 46−82% yields and 38−72% ee (entries 1−9 of Table S5 in Supporting Information). Similarly, the same reaction catalyzed by *trans*-$[Ru^{II}(salen^A)(NO)(Cl)]$ (salen = $salen^{A9}$−$salen^{A11}$) was previously reported to give **4a** in 54−66% yields and 67−82% ee[18a,c] (Table S5 in Supporting Information).

Given the markedly different enantiocontrol in the intramolecular cyclopropanation of allylic diazoacetates catalyzed by the ruthenium complexes with $salen^A$ ligands in planar and nonplanar coordination modes, we propose that a *cis*-*β*-ruthenium−carbene intermediate is involved in the **1a**−**c**-catalyzed reactions. Our attempts to identify such intermediates by spectroscopic means have not been successful; therefore, we performed DFT calculations on the model complexes depicted in Chart 1, which are possibly involved in the intramolecular

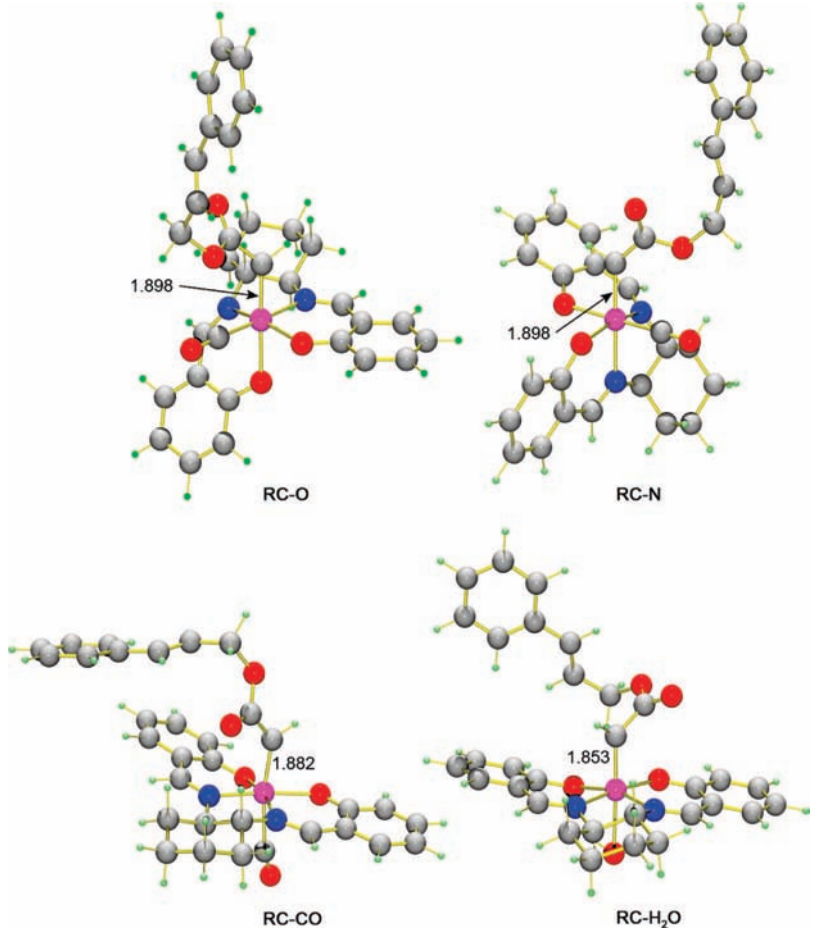

Figure 5. Calculated structures of **RC-O**, **RC-N**, **RC-CO**, and **RC-H$_2$O**. The Ru−C(carbene) distances (Å) are indicated.

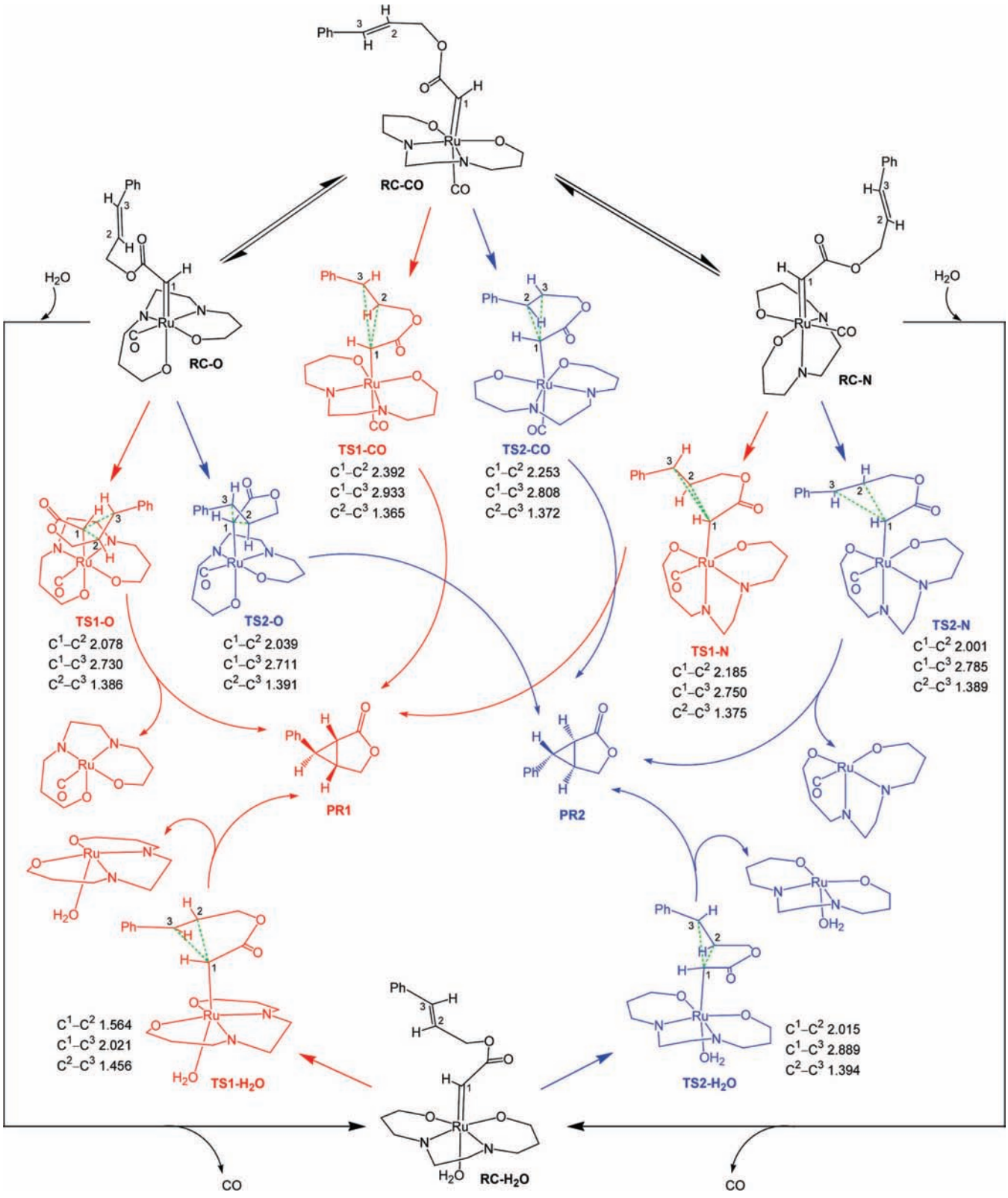

Figure 6. Schematic diagram showing the reaction routes based on **RC-O**, **RC-N**, **RC-CO**, and **RC-H_2O**. The calculated distances (Å) of C^1-C^2, C^1-C^3, and C^2-C^3 bonds in the transition states **TS1** and **TS2** are indicated. For the calculated structures of the carbene intermediates and their transition states, see Figure 5 and Figure S3 in the Supporting Information.

cyclopropanation of **3a** mediated by model complex *cis*-β-$[Ru^{II}(salen^{A0})(CO)_2]$.

For the key bond lengths of the calculated **RC-O** or **RC-N** species, there is good agreement between the B3LYP results

(32) Doyle, M. P.; Zhou, Q.-L.; Dyatkin, A. B.; Ruppar, D. A. *Tetrahedron Lett.* **1995**, *36*, 7579.

(33) Park, S.-B.; Murata, K.; Matsumoto, H.; Nishiyama, H. *Tetrahedron: Asymmetry* **1995**, *6*, 2487.

Table 3. Relative Energies and Free Energies (kcal/mol) for the Reactions Based on **RC-O**, **RC-N**, **RC-CO**, and **RC-H_2O**

system	ΔE	ΔG
RC-O	0.0	0.0
TS1-O	9.7	11.6
TS2-O	11.7	13.8
RC-N	2.1	0.5
TS1-N	9.7	11.6
TS2-N	15.7	17.2
RC-CO	3.8	3.9
TS1-CO	12.7	15.8
TS2-CO	14.2	17.0
PR1	−16.4	−28.6
PR2	−16.4	−28.5
RC-H_2O	0.0	0.0
TS1-H_2O	15.4	19.4
TS2-H_2O	17.6	22.5
PR1	25.2	14.7
PR2	25.3	14.8

and related experimental values. For instance, the Ru−C (carbene) bond lengths of 1.898 Å for **RC-O** and **RC-N** (Figure 5) are consistent with those of 1.910(2)−1.921(12) Å in structurally characterized ruthenium−carbene complexes *trans*-[Ru^{II}($salen^{A}$)(CAr_2)(py)] and *trans*-[Ru^{II}($salen^{A}$)(CAr_2)(MeIm)] reported previously.[6] The Ru−C(CO) bond lengths in **RC-O** (1.916 Å) and **RC-N** (1.887 Å) compare well with those in the crystal structures of **1a**,**c**. This lends credence to our B3LYP calculations, which provide an adequate theoretical level for the investigation of molecular geometries, electronic structures, and kinetic features of the reactions.

According to the results depicted in Table 3, **RC-CO** is less stable than **RC-O** and **RC-N** by 3.9 and 3.4 kcal/mol, respectively. These differences in free energy are relatively small, suggesting a possible equilibrium between the *trans* and *cis*-β intermediates, as depicted in Figure 6. The enthalpy change from **RC-O** to **RC-H_2O** by ligand exchange of CO with H_2O was calculated to be 2.3 kcal/mol, indicating a higher stability of **RC-O** and **RC-N** than **RC-H_2O**, although the *trans* species **RC-H_2O** is more stable by 2−4 kcal/mol compared with *cis*-β-**RC-H_2O** species (structures not shown in Chart 1). Thus, the major carbene intermediates in the reaction would be the *cis*-β species **RC-O** and **RC-N**, with the former being slightly more stable by 0.5 kcal/mol.

Inspection of Figure 6 revealed that **RC-O**, **RC-N**, **RC-CO**, and **RC-H_2O** each undergo intramolecular cyclopropanation to give enantiomers **PR1** and **PR2** of **4a** via the corresponding transition states **TS1** and **TS2**, respectively, by an asynchronous concerted [2 + 1] addition mechanism, with the C^1 atom of the singlet carbene group initially attacking only the C^2 atom of the alkene group[35] (note the significantly shorter C^1−C^2 distance than the C^1−C^3 distance in each structure of the transition states). A similar asynchronous approach has previously been found for the addition of a singlet carbene to ethylene.[36]

As the reaction goes from the reactant to the transition state, the distance between the C^2 and C^3 atoms is elongated from 1.347 to 1.386 (**TS1-O**), 1.391 (**TS2-O**), 1.375 (**TS1-N**), 1.389 (**TS2-N**), 1.365 (**TS1-CO**), and 1.372 Å (**TS2-CO**). These changes can be mainly attributed to the interaction of the C^1 atom with the π orbital of C^2−C^3 double bond associated with a slight elongation of the C^2−C^3 bond. The angles of C^2−C^1−H are 100.2, 101.3, 99.7, 96.9, 96.0, and 91.0° for the transition states **TS1-O**, **TS2-O**, **TS1-N**, **TS2-N**, **TS1-CO**, and **TS2-CO**, respectively. On the basis of these changes in bond distances and angles, the cyclopropanation reactions of **RC-O**, **RC-N**, and **RC-CO** have early transition states close to the reactants.

The calculated free energies of activation for **TS1** (**TS1-O**, 11.6; **TS1-N**, 11.5; **TS1-CO**, 15.8 kcal/mol) are smaller than those for **TS2** (**TS2-O**, 13.8; **TS2-N**, 17.5; **TS2-CO**, 17.0 kcal/mol), revealing that the formation of **PR1** is more favorable than that of **PR2**. Thus, **PR1** would be the major enantiomer, whereas **PR2** is the minor enantiomer, consistent with the results obtained for the formation of **4a** through **1a**-catalyzed cyclopropanation of **3a**. Since the ΔG value for **TS1-N** is identical to that for **TS1-O** (Table 3), and **RC-N** is only slightly less stable than **RC-O**, the formation of **PR1** from **RC-N** could compete with that from **RC-O**. Both pathways are more favorable than that involving **RC-CO** and **TS1-CO**, owing to the lower stability of **RC-CO** than **RC-O** and **RC-N** as mentioned above.

For the cyclopropanation of **RC-H_2O** (an endothermic process), the free energies of activation, 19.4 kcal/mol for **TS1-H_2O** and 22.5 kcal/mol for **TS2-H_2O** (Table 3), are quite high, and the corresponding free energies are 14.7 and 14.8 kcal/mol, respectively, in contrast to those of −28.6 and −28.5 kcal/mol for the cyclopropanation of **RC-O** (an exothermic process). A late transition state was found for the asynchronous approach for the reaction involving the **RC-H_2O** species, as shown from the C^1−C^2 and C^2−C^3 distances of 1.564 and 1.456 Å in **TS1-H_2O** (Figure 6). Such higher free energies of activation (19.4 kcal/mol), coupled with a late transition state, for the cyclopropanation of **RC-H_2O** would render this reaction an unfavorable pathway.

On the basis of the difference in ΔG between **TS1** and **TS2**, the enantioselectivity of the cyclopropanation was predicted to be 77% ee for the *trans* species **RC-CO** and 96% ee for the *cis*-β species **RC-O**. To estimate the steric effect, full models formed by replacing the $salen^{A0}$ of **RC-CO** and **RC-O** with $salen^{A1}$ were calculated, and the predicted ee values are 98 and 99%, respectively. Changing the basis set from 6-31G to 6-31G(d,p) resulted in a small change in the energy difference between **TS1-O** and **TS2-O** from 2.71 to 2.49 kcal/mol, the latter corresponding to an ee value of 98%. When solvent effect was considered, single-point energy calculations performed at the B3LYP/PCM/6-31G(d,p)//B3LYP/6-31G level of theory gave an energy difference of 2.75 kcal/mol (99% ee) between **TS1-O** and **TS2-O**. Such small changes in the energy difference between **TS1-O** and **TS2-O** under different conditions indicate that the results based on our calculation condition are reliable. The calculated ee values of 98−99% are in excellent agreement with the experimental ee value of 98% found for catalyst **1a** (entry 1 in Table 2).

So what is the role of a nonplanar coordination mode of salen ligand? This allows the isolation of an air-stable [Ru^{II}($salen^{A1}$)($CO)_2$] (**1a**) containing the sterically encumbered Jacobsen's salen ligand. The *cis*-β-[Ru^{II}($salen^{A}$)($CO)_2$] can generate a *cis*-β-ruthenium−carbene intermediate featuring high

(34) Che, C.-M.; Huang, J.-S.; Lee, F.-W.; Li, Y.; Lai, T.-S.; Kwong, H.-L.; Teng, P.-F.; Lee, W.-S.; Lo, W.-C.; Peng, S.-M.; Zhou, Z.-Y. *J. Am. Chem. Soc.* **2001**, *123*, 4119.

(35) The attack of C^3 by C^1 would be an unfavorable pathway due to the steric hindrance of the phenyl group. See: Fang, R.; Ke, Z.; Shen, Y.; Zhao, C.; Phillips, D. L. *J. Org. Chem.* **2007**, *72*, 5139.

(36) (a) Rondan, N. G.; Houk, K. N.; Moss, R. A. *J. Am. Chem. Soc.* **1980**, *102*, 1770. (b) Houk, K. N.; Rondan, N. G.; Mareda, J. *J. Am. Chem. Soc.* **1984**, *106*, 4291. (c) Blake, J. F.; Wierschke, S. G.; Jorgenson, W. L. *J. Am. Chem. Soc.* **1989**, *111*, 1919. (d) Keating, A. E.; Garcia-Garibay, M. A.; Houk, K. N. *J. Am. Chem. Soc.* **1997**, *119*, 10805. (e) Bernardi, F.; Bottoni, A.; Canepa, C.; Olivucci, M.; Robb, M. A.; Tonachini, G. *J. Org. Chem.* **1997**, *62*, 2018.

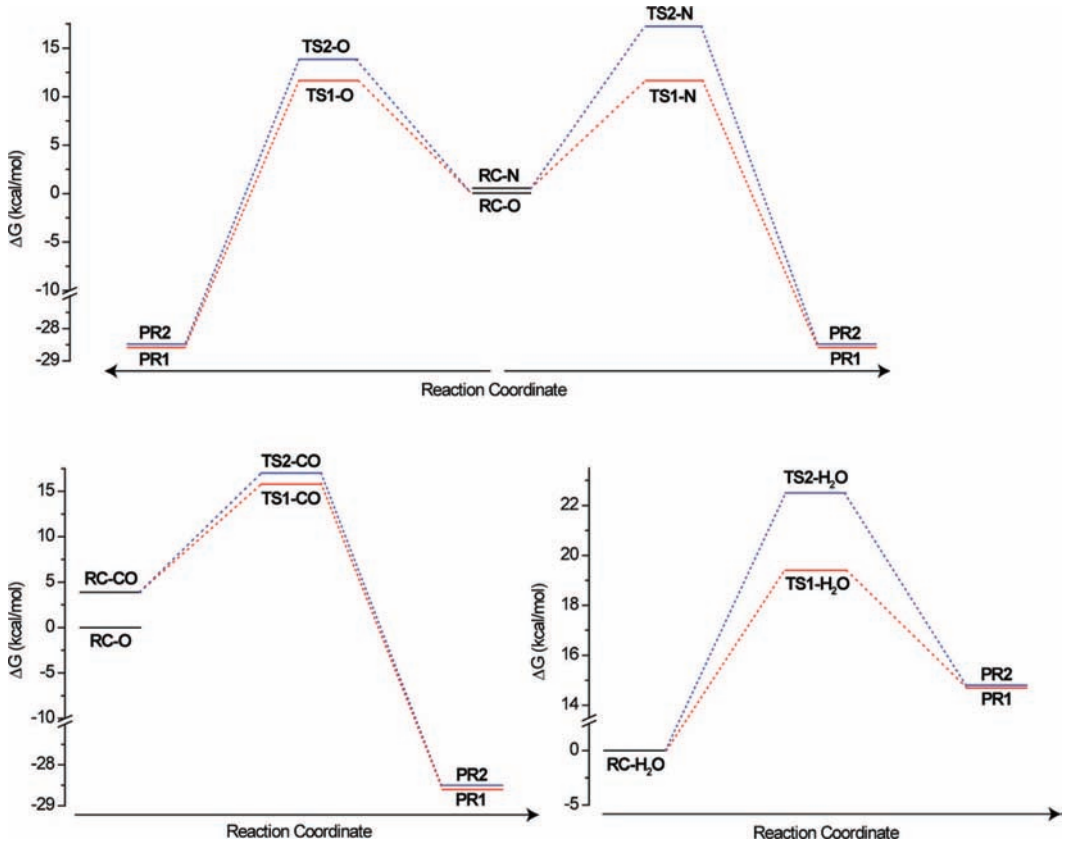

Figure 7. Free energy profiles for the cyclopropanation reactions based on **RC-O**, **RC-N**, **RC-CO**, and **RC-H$_2$O**.

enantiocontrol and requiring smaller free energy of activation than the *trans* counterparts to undergo intramolecular cyclopropanation. According to the DFT calculations, the ee value for the *cis-β*-ruthenium−carbene intermediate such as **RC-O** is insensitive to the substituent on the salen^{A} ligand, in contrast to an increase in ee from 77 to 98% for the *trans* counterpart **RC-CO** upon changing salen^{A0} to salen^{A1}. The observed variation in ee values for **1a**−**c** (90−98%, Table 1) can be rationalized by the existence of an equilibrium between *cis-β* (major) and *trans* (minor) ruthenium−carbene intermediates. Such equilibrium, however, does not affect the ee value for catalyst **1a** (under *hν*) since both the *cis-β*- and *trans*-carbene intermediates in this case feature high ee values for the conversion of **3a** to **4a**.

Conclusion

We have isolated and structurally characterized several ruthenium(II) complexes, *cis-β*-[Ru(salen^{A})(CO)$_2$], bearing 1,2-diamine-derived salen ligands in a nonplanar coordination mode. These complexes are highly selective catalysts for intramolecular cyclopropanation of *trans*-allylic diazoacetates under light irradiation, with the cyclopropanation products obtained in up to 96% yield and up to 98% ee. DFT calculations on the intramolecular cyclopropanation of **3a** catalyzed by *cis-β*-[Ru(salen^{A0})(CO)$_2$] revealed that, among the ruthenium−carbene intermediates possibly involved in the reactions, the *cis-β* species **RC-O** and **RC-N** are more stable than their *trans* isomer **RC-CO** bearing salen^{A0} in a planar coordination mode, and the intramolecular cyclopropanation from these *cis-β* species is the most favorable pathway. The present work, together with recent DFT calculations by Morokuma and co-workers for Mn−salen^{A}-catalyzed alkene oxidation,[5] implies that a nonplanar coordination mode of salen^{A} ligand including Jacobsen's salen ligand can be used for the design of new metal catalysts for highly enantioselective carbenoid transfer reactions.

Experimental Section

General. All solvents were dried and distilled under argon atmosphere according to standard procedures. Commercially available reagents were used as received unless otherwise specified. Compounds (1*R*,2*R*)-H$_2$salen^{A1},[37] (1*R*,2*R*)-H$_2$salen^{A3},[38] *rac*-H$_2$salen^{B1},[39] **3a**,[9b] **3b**,**c**,**e**,[18c] and **3h**,**i**[9b] were prepared by literature methods. ^{1}H NMR spectra were recorded on a Bruker AM300, AM400, or a Varian Mercury 300 spectrometer (with SiMe$_4$ as an internal reference). IR measurements were performed as KBr disks on a Bio-Rad FTS-185 spectrometer. Optical rotations were determined on a Perkin-Elmer 341MC polarimeter at 589 nm and 20 °C. Mass spectra were measured on a HP5989A or an Aglient HP5873 spectrometer. High-resolution mass spectra were obtained on a Kratos Concept 1H spectrometer. Elemental analyses were performed on an Elemantar Vario EL instrument at the Analytical and Testing Center, Shanghai Institute of Organic Chemistry, Chinese Academy of Sciences. Enantioselectivities were determined on a Waters 5151 HPLC equipped with a Chiralpak OA column.

Preparation of (1*R*,2*R*)-H$_2$salen^{A2}. This compound was prepared by the same method as that for (1*R*,2*R*)-H$_2$salen^{A1}:[37] $[\alpha]^{20}_{D}$ −440.6 (c = 1.33, CH_2Cl_2); ^{1}H NMR ($CDCl_3$, 300 MHz) δ 13.68 (s, 2H), 8.28 (s, 2H), 7.20−7.18 (m, 2H), 7.01−6.98 (m, 2H), 6.79−6.74 (m, 2H), 3.44−3.30 (m, 4H), 1.96−1.43 (m, 8H), 1.23−1.20 (m, 12H); HRMS calcd for $C_{26}H_{34}N_2O_2$ (M^+) 406.2620, found 406.2614.

Preparation of *rac*-H$_2$salen^{B2}. This compound was prepared by the same method as that for *rac*-H$_2$salen^{B1}:[39] ^{1}H NMR ($CDCl_3$, 300

(37) Deng, Li; Jacobsen, E. N. *J. Org. Chem.* **1992**, *57*, 4320.
(38) Belokon, Y.; Ikonnikov, N.; Moscalenko, M.; North, M.; Orlova, S.; Tararov, V.; Yashkina, L. *Tetrahedron: Asymmetry* **1996**, *7*, 851.
(39) Takenaka, N.; Huang, Y.; Rawal, V. H. *Tetrahedron* **2002**, *58*, 8299.

MHz) δ 12.40 (s, 2H), 8.56 (s, 2H), 8.05 (d, $J = 9.0$ Hz, 2H), 7.95 (d, $J = 8.1$ Hz, 2H), 7.55 (d, $J = 9.0$ Hz, 2H), 7.47−7.41 (m, 2H), 7.30−7.27 (m, 4H), 7.14 (d, $J = 8.1$ Hz, 2H), 7.00−6.97 (m, 2H), 6.77−6.71 (m, 2H), 3.14−3.05 (m, 2H), 1.13−1.05 (m, 12H); HRMS calcd for $C_{40}H_{37}N_2O_2$ ($M + H^+$) 577.2855, found 577.2842.

Preparation of *cis*-β-[Ru^{II}(salen^{A})$(CO)_2$] (1). To a degassed flask equipped with a condenser were added $Ru_3(CO)_{12}$ (0.57 mmol) and (1*R*,2*R*)-H_2salen^{A} (0.57 mmol) under argon atmosphere, followed by addition of 1,2,4-trichlorobenzene (5 mL). The mixture was stirred at 190−195 °C for 6 h and then cooled to room temperature. Upon flash chromatography on silica gel with petroleum ether/ethyl acetate (5:1 v/v) as eluent, the product was recrystallized from dichloromethane/methanol and dried.

***cis*-β-[Ru^{II}(salen^{A1})$(CO)_2$] (1a):** Yield 30%; ^{1}H NMR ($CDCl_3$, 400 MHz) δ 8.28 (d, $J = 1.6$ Hz, 1H), 7.97 (s, 1H), 7.42 (d, $J = 2.7$ Hz, 1H), 7.34 (d, $J = 2.7$ Hz, 1H), 6.99 (d, $J = 2.6$ Hz, 1H), 6.96 (d, $J = 2.7$ Hz, 1H), 3.58−3.50 (m, 1H), 3.05−2.97 (m, 1H), 2.74−2.70 (m, 1H), 2.35−2.31 (m, 1H), 2.05−1.99 (m, 2H), 1.86−1.78 (m, 1H), 1.67−1.59 (m, 1H), 1.56−1.41 (m, 2H), 1.38 (s, 9H), 1.34 (s, 9H), 1.31 (s, 9H), 1.29 (s, 9H); IR 2040, 1965 cm^{-1} (ν(CO)); FAB MS *m*/*z* 702 (M^+). Anal. Calcd for $C_{38}H_{52}N_2O_4Ru$: C, 65.02; H, 7.47; N, 3.99. Found: C, 64.83; H, 7.11; N, 3.74.

***cis*-β-[Ru^{II}(salen^{A2})$(CO)_2$] (1b):** Yield 34%; ^{1}H NMR ($CDCl_3$, 300 MHz) δ 8.32 (s, 1H), 8.02 (s, 1H), 7.24−7.20 (m, 2H), 7.09−7.05 (m, 2H), 6.64−6.52 (m, 2H), 3.71−3.64 (m, 1H), 3.51−3.38 (m, 2H), 3.18−3.11 (m, 1H), 2.77−2.71 (m, 1H), 2.40−2.35 (m, 1H), 2.09−2.04 (m, 2H), 1.86−1.85 (m, 1H), 1.68−1.63 (m, 1H), 1.50−1.40 (m, 2H), 1.26−1.13 (m, 12H); IR 2034, 1959 cm^{-1} (ν(CO)); FAB MS *m*/*z* 562 (M^+). Anal. Calcd for $C_{28}H_{32}N_2O_4Ru$: C, 59.88; H, 5.74; N, 4.99. Found: C, 60.14; H, 5.85; N, 4.72.

***cis*-β-[Ru^{II}(salen^{A3})$(CO)_2$] (1c):** Yield 37%. ^{1}H NMR ($CDCl_3$, 300 MHz) δ 8.33 (s, 1H), 8.00 (s, 1H), 7.36−7.32 (m, 1H), 7.29−7.27 (m, 1H), 7.12−7.09 (m, 2H), 6.58−6.51 (m, 2H), 3.62−3.54 (m, 1H), 3.11−3.05 (m, 1H), 2.75−2.71 (m, 1H), 2.39−2.33 (m, 1H), 2.06−1.99 (m, 2H), 1.88−1.81 (m, 1H), 1.70−1.65 (m, 1H), 1.47−1.37 (m, 2H), 1.36 (s, 9H), 1.33 (s, 9H); IR 2042, 1958 cm^{-1} (ν(CO)); FAB MS *m*/*z* 590 (M^+). Anal. Calcd for $C_{30}H_{36}N_2O_4Ru$: C, 61.10; H, 6.15; N, 4.75. Found: C, 60.79; H, 6.07; N, 4.52.

Preparation of *cis*-β-[Ru^{II}(salen^{B})$(CO)_2$] (2). To a degassed flask equipped with a condenser were added $Ru_3(CO)_{12}$ (0.35 mmol) and the corresponding racemic Schiff base ligand (0.35 mmol) under argon atmosphere, followed by addition of 1,2,4-trichlorobenzene (5 mL). The mixture was stirred at 190−195 °C for 6 h and, after being cooled to room temperature, was subjected to flash chromatography on silica gel with petroleum ether/ethyl acetate (10:1 v/v) as eluent. The eluate was evaporated in vacuo, and the residue was dissolved in CH_2Cl_2 (0.1 mL). Addition of hexane (30 mL) resulted in precipitation of the product. The precipitate was collected by filtration and recrystallized from CH_2Cl_2/MeOH to give **2** as a yellow crystalline solid.

***cis*-β-[Ru^{II}(salen^{B1})$(CO)_2$] (2a):** Yield 16%; ^{1}H NMR ($CDCl_3$, 300 MHz) δ 8.13 (s, 1H), 8.08−8.04 (m, 1H), 7.98−7.95 (m, 1H), 7.84−7.80 (m, 2H), 7.56 (s, 1H), 7.53−7.30 (m, 5H), 7.22−7.10 (m, 4H), 6.94−6.89 (m, 2H), 6.58 (s, 1H), 1.35 (s, 18H), 1.24 (s, 9H), 1.15 (s, 9H); IR 2046, 1977 cm^{-1} (ν(CO)); FAB MS *m*/*z* 872 (M^+).

***cis*-β-[Ru^{II}(salen^{B2})$(CO)_2$] (2b):** Yield 40%; ^{1}H NMR ($CDCl_3$, 300 MHz) δ 8.15 (s, 1H), 8.07−8.05 (m, 1H), 7.98−7.95 (m, 1H), 7.81−7.79 (m, 2H), 7.56 (s, 1H), 7.52−7.47 (m, 1H), 7.41−7.30 (m, 3H), 7.21−7.09 (m, 5H), 7.01−6.99 (m, 1H), 6.92−6.89 (m, 1H), 6.68−6.64 (m, 1H), 6.53−6.48 (m, 1H), 6.37−6.31 (m, 1H), 3.35−3.27 (m, 2H), 1.22−1.14 (m, 12H); IR 2048, 1973 cm^{-1} (ν(CO)); FAB MS 732 (M^+). Anal. Calcd for $C_{42}H_{34}N_2O_4Ru$: C, 68.93; H, 4.68; N, 3.83. Found: C, 68.82; H, 4.88; N, 3.78.

Preparation of Allylic Diazoacetates 3d,f,g. To a mixture of (*E*)-3-R-2-propen-1-yl acetoacetate (1.49 mmol; R = 4-tolyl for **3d**, 2-tolyl for **3f**, 2-furanyl for **3g**), MeCN (5 mL), and Et_3N (164 mg, 1.62 mmol) was added, dropwise, a solution of TsN_3 (292 mg, 1.49 mmol) in MeCN (5 mL). The resulting mixture was stirred at room temperature for 5 h and then treated with a solution of LiOH (184 mg, 4.4 mmol) in H_2O (5 mL). Upon stirring for 7 h, the mixture was diluted with saturated aqueous NaCl solution (15 mL) and extracted with Et_2O (20 mL × 3). The organic phases were combined, washed with saturated aqueous NaCl solution, and dried with Na_2SO_4. Chromatography on silica gel H with petroleum ether/ethyl acetate (10:1 v/v) afforded the desired product **3**.

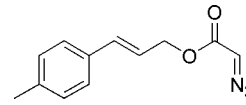

3d: Yield 68%; ^{1}H NMR ($CDCl_3$, 300 MHz) δ 7.30−7.27 (m, 2H), 7.15−7.12 (m, 2H), 6.65−6.60 (m, 1H), 6.29−6.19 (m, 1H), 4.83−4.79 (m, 3H), 2.34 (s, 3H); IR 2110, 1692, 1513, 1389, 1352, 1238, 1176, 968 cm^{-1}; HRMS calcd for $C_{12}H_{12}N_2O_2$ (M^+) 216.0899, found 216.0904.

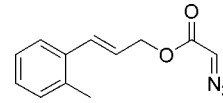

3f: Yield 59%; ^{1}H NMR ($CDCl_3$, 300 MHz) δ 7.44−7.36 (m, 1H), 7.17−7.13 (m, 3H), 6.90−6.86 (m, 1H), 6.22−6.13 (m, 1H), 4.85−4.79 (m, 3H), 2.36 (s, 3H); IR 2110, 1692, 1485, 1459, 1390, 1352, 1238, 1177, 966, 740 cm^{-1}; HRMS cacld for $C_{12}H_{12}N_2O_2$ (M^+) 216.0899, found 216.0907.

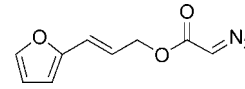

3g: Yield 49%; ^{1}H NMR ($CDCl_3$, 300 MHz) δ 7.36 (s, 1H), 6.46 (d, $J = 15.9$ Hz, 1H), 6.39−6.36 (m, 1H), 6.29 (d, $J = 3.3$ Hz, 1H), 6.25−6.16 (m, 1H), 4.80−4.77 (m, 3H); IR 2112, 1691, 1390, 1350, 1240, 1178, 1013, 961, 738 cm^{-1}; HRMS calcd for $C_9H_8N_2O_3$ (M^+) 192.0535, found 192.0537.

General Procedure for the *cis*-β-[Ru^{II}(salen)$(CO)_2$]-Catalyzed Intramolecular Cyclopropanation of Allylic Diazoacetates. To a degassed Schlenk tube equipped with a condenser were added the diazo compound (0.25 mmol) and catalyst **1** (1 mol %) under argon atmosphere, followed by addition of CH_2Cl_2 (3 mL) containing methanol (0.03% v/v). The mixture was refluxed for 3−5 h under irradiation with an incandescent lamp (300 W) or for 18 h in the dark and then subjected to flash chromatography on silica gel with petroleum ether/ethyl acetate (5:1 v/v) as eluent. The eluate was evaporated to dryness in vacuo to give the cyclopropanation product as a white solid.

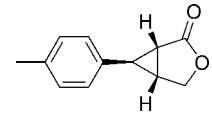

4d: ^{1}H NMR ($CDCl_3$, 300 MHz) δ 7.12 (d, $J = 7.8$ Hz, 2H), 6.96 (d, $J = 7.8$ Hz, 2H), 4.49−4.39 (m, 2H), 2.53−2.48 (m, 1H), 2.32 (s, 3H), 2.31−2.28 (m, 2H); IR 1765, 1518, 1171, 1036, 970, 870, 806 cm^{-1}; HRMS calcd for $C_{12}H_{12}O_2$ (M^+) 188.0837, found 188.0840.

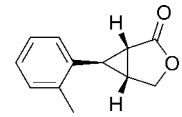

4f: ^{1}H NMR ($CDCl_3$, 300 MHz) δ 7.23−7.17 (m, 1H), 7.08−7.05 (m, 1H), 6.88−6.85 (m, 2H), 4.49−4.39 (m, 2H), 2.55−2.50 (m, 1H), 2.35 (s, 3H), 2.34−2.28 (m, 2H); IR 1770, 1493, 1460, 1369,

1175, 1037, 973, 756 cm^{-1}; HRMS calcd for $C_{12}H_{12}O_2$ (M^+) 188.0837, found 188.0835.

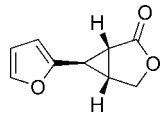

4g: ^1H NMR ($CDCl_3$, 300 MHz) δ 7.29−7.28 (m, 1H), 6.32−6.30 (m, 1H), 6.16−6.14 (m, 1H), 4.48−4.37 (m, 2H), 2.67−2.62 (m, 1H), 2.45−2.42 (m, 1H), 2.37−2.35 (m, 1H); IR 1768, 1371, 1174, 1037, 969 cm^{-1}; HRMS calcd for $C_9H_8O_3$ (M^+) 164.0473, found 164.0472.

For characterization of **4a**,[9b] **4b**,**c**,**e**,[18c] and **4h**,**i**,[9b] see the references indicated.

X-ray Crystal Structure Determinations. Diffraction-quality crystals of **1a**·3MeOH, **1c**, and **2a**·0.5CH_2Cl_2 were obtained by slow evaporation of the solutions in CH_2Cl_2/MeOH. A crystal of dimensions 0.3 × 0.2 × 0.15 mm^3 for **1a**·3MeOH, 0.6 × 0.3 × 0.25 mm^3 for **1c**, and 0.5 × 0.4 × 0.25 mm^3 for **2a**·0.5CH_2Cl_2 mounted in a glass capillary was used for data collection at 28 °C on a MAR diffractometer with a 300 mm image plate detector using graphite monochromatized Mo Kα radiation (λ = 0.71073 Å). Data collection was made with 2° oscillation step of φ, 900 (**1a**·3MeOH), 420 (**1c**), and 600 s (**2a**·0.5CH_2Cl_2) exposure time, and 120 mm scanner distance, with 88 images for **1a**·3MeOH and 100 images for each of **1c** and **2a**·0.5CH_2Cl_2 being collected. The images were interpreted, and intensities were integrated using program DENZO.[40] The structure was solved by direct methods by employing SHELXS-97[41] (**1a**·3MeOH) or SIR-97[42] (**1c**, **2a**·0.5CH_2Cl_2) program on a PC. Ru and many non-hydrogen atoms were located according to the direct methods. The positions of the other non-hydrogen atoms were found after successful refinement by full-matrix least-squares using program SHELXL-97[43] on a PC. The positions of H atoms were calculated based on riding mode with thermal parameters equal to 1.2 times that of the associated C atoms and participated in the calculation of final *R* indices. For **1a**·3MeOH, one crystallographic asymmetric unit consists of one formula unit and three methanol molecules, and one of the *tert*-butyl groups was disordered by rotation along the C−C bond and was treated in two sets of positions of the methyl groups; in the final stage of least-squares refinement, only Ru atom, the atoms of the two CO groups, and the other atoms coordinated to Ru were refined anisotropically; other non-hydrogen atoms were refined isotropically. For **1c**, one crystallographic asymmetric unit consists of one formula unit; in the final stage of least-squares refinement, all non-hydrogen atoms were refined anisotropically. In the case of **2a**·0.5CH_2Cl_2, one crystallographic asymmetric unit consists of two formula units, including one dichloromethane solvent molecule; each formula unit contains one disordered *tert*-butyl group in the mode of rotation; in the final stage of least-squares refinement, non-hydrogen atoms of disordered groups were refined isotropically; other non-hydrogen atoms were refined anisotropically.

Computational Details. The intramolecular cyclopropanation of diazoacetate **3a** catalyzed by **1a** was investigated as a basic model reaction. To keep the computational cost low, all the ^{t}Bu groups in **1a** were replaced with a simple H atom in the calculation, unless otherwise indicated. Geometries, energies, and first- and second-energy derivatives of all stationary points were fully optimized by hybrid density functional theory (DFT) using the GAUSSIAN 03 program suite.[44] For the DFT calculations, we used the hybrid gradient-corrected exchange functional of Lee, Yang, and Parr.[45] This functional is commonly known as B3LYP and has been shown to be quite reliable for computing geometries.[46] The 6-31G[47] basis set was selected for all atoms except ruthenium, for which the effective core potential of Hay and Wadt (LANL2DZ)[48] was used both to accurately take relativistic effects into account and to substantially reduce the number of electrons in the system. Vibrational frequency calculations at the B3LYP/6-31G level of theory were used to characterize all of the stationary points as either minima (the number of imaginary frequencies (NIMAG = 0) or transition states (NIMAG = 1)). The relative energies are, thus, corrected for vibrational zero-point energies (ZPE, not scaled). The solvent effect on the reaction was considered by applying the polarized continuum model (PCM),[49] with single-point energy calculations being performed at the B3LYP/PCM/6-31G(d,p)//B3LYP/6-31G level of theory using the geometries along the minimum energy pathway. The dielectric constant for the bulk dichloromethane was assumed to be 8.93. Intrinsic reaction coordinate (IRC)[50] calculations were performed to unambiguously connect the transition states with reactants and the products. The detailed structural parameters and energies determined for the model carbene intermediates and transition states are listed in Table S6 in Supporting Information.

Acknowledgment. This work was supported by The University of Hong Kong (University Development Fund), the Hong Kong Research Grants Council (HKU 7012/05P), and the University Grants Committee of the Hong Kong SAR of China (Area of Excellent Scheme, AoE/P-10/01). We are grateful to the reviewers for their invaluable suggestions. C.Y.Z. thanks the support of the National Natural Science Foundation of China (Grant No. 20673149).

Supporting Information Available: A complete list of authors for ref 44. Tables S1−S6, Figures S1−S5, HPLC diagrams for **4a**−**i**, and CIF files for **1a**,**c** and **2a**. This material is available free of charge via the Internet at http://pubs.acs.org.

JA8086399

(40) Otwinowski, Z.; Minor, W. In *Methods in Enzymology: Macromolecular Crystallography*; Part A., Carter, C. W., Jr., Sweet, R. M., Eds.; Academic Press: New York, 1997; Vol. 276, p 307.
(41) Sheldrick, G. M. *SHELXS-97. Program for the Solution of Crystal Structures*; University of Göttingen: Göttingen, Germany, 1997.
(42) Altomare, A.; Burla, M. C.; Camalli, M.; Cascarano, G. L.; Giacovazzo, C.; Guagliardi, A.; Moliterni, A. G. G.; Polidori, G.; Spagna, R. *J. Appl. Crystallogr.* **1999**, *32*, 115.
(43) Sheldrick, G. M. *SHELXL-97. Program for the Refinement of Crystal Structures*; University of Göttingen: Göttingen, Germany, 1997.
(44) Frisch, M. J.; *Gaussian 03*, revision D.01; Gaussian, Inc.: Wallingford CT, 2004.
(45) Lee, C.; Yang, W.; Parr, R. G. *Phys. Rev. B* **1988**, *37*, 785.
(46) (a) Jursic, B.; Zdravkovski, Z. *J. Chem. Soc., Perkin Trans. 2* **1995**, 1223. (b) Jursic, B. S. *Chem. Phys. Lett.* **1996**, *256*, 603. (c) Jursic, B. S. *J. Mol. Struct. (THEOCHEM)* **1998**, *425*, 193. (d) Jursic, B. S. *J. Mol. Struct. (THEOCHEM)* **1998**, *452*, 145.
(47) (a) Rassolov, V. A.; Ratner, M. A.; Pople, J. A.; Redfern, P. C.; Curtiss, L. A. *J. Comput. Chem.* **2001**, *22*, 976. (b) Rassolov, V. A.; Pople, J. A.; Ratner, M. A.; Windus, T. L. *J. Chem. Phys.* **1998**, *109*, 1223.
(48) Hay, P. J.; Wadt, W. R. *J. Chem. Phys.* **1985**, *82*, 299.
(49) Foresman, J. B.; Keith, T. A.; Wiberg, K. B.; Snoonian, J.; Frisch, M. J. *J. Phys. Chem.* **1996**, *100*, 16098.
(50) Gonzalez, C.; Schlegel, H. B. *J. Chem. Phys.* **1989**, *90*, 2154.